The self-consistent band structure of PtSSe by the linear muffin-tin orbital method in the atomic sphere approximation

The self-consistent band structure of PtSSe by the linear muffin-tin orbital method in the atomic sphere approximation

C Mankai and H Romdhani

Laboratoire de la Matière Condensée, Département de Physique, Faculté des Sciences de Tunis, Campus Universitaire 1060 Tunis, Tunisia

Abstract.   The self-consistent band structure and the density of states of the layer compound PtSSe were calculated using the linear muffin-tin orbital method in the atomic sphere approximation (LMTO-ASA). This calculation includes the relativistic mass–velocity and Darwin terms but excludes the spin–orbit coupling. The Barth–Hedin local exchange correlation potential was used. The result, reported for the first time, predicts that PtSSe is a semiconductor with an energy gap of about 0.64 eV. Such a behaviour is confirmed by the experimental data available. The self-consistent band structure of PtS_2 and $PtSe_2$ were calculated, by the same method, and the effect of the anion substitution in the sequence $PtS_2 \rightarrow PtSSe \rightarrow PtSe_2$ have been studied. The results are discussed in terms of charge transfer and local coordination of the constituent atoms.

1. Introduction

PtSSe is layer compound with a CdI_2-type Bravais lattice having the space group $P31m$ [1]. The structural units of PtSSe are composed of platinum atoms in octahedral holes sandwiched between two close-packed planes of chalcogene atoms: a plane of sulfur and another of selenium. Whereas the bonding, inside a layer, between the platinum and the sulfur and selenium atoms is expected to present a mixed covalent ionic character. Adjacent layers are held together mainly by van der Waals forces which give a lamellar structure to this compound.

The layered transition metal dichalcogenides of type TX_2 have been studied extensively and several theoretical results and experimental data are available [2, 3]. It is not the case for the type TXY such as PtSSe, where a few electrical and optical data are available [4]. From galvanomagnetic properties this compound exhibits a semiconductor behaviour [5].

The aim of this paper is to determine the band structure of PtSSe and to study the effect of the anion substitution in the sequence $PtS_2 \rightarrow PtSSe \rightarrow PtSe_2$. For this purpose, the band structure of PtS_2 and $PtSe_2$ have been calculated.

Combining the difference in the chemical properties of sulfur and selenium atoms in the PtSSe, with the layer character of its structure, we expected a very peculiar band structure for this compound. Moreover, the difference between the lattice constants of the three compounds PtS_2, PtSSe and $PtSe_2$, and the substitution of only one anion at a time, in the sequence $PtS_2 \rightarrow PtSSe \rightarrow PtSe_2$ may be useful for understanding the nature and the character of the intra-layer and inter-layer bonding.

The plan of this paper is as follows. In section 2 we briefly outline the method of calculation. The results of the band structure, the corresponding density of states and discussion will be the subject of section 3. In section 4 we discuss, in the sequence $PtS_2 \rightarrow PtSSe \rightarrow PtSe_2$ and the effect of substitution of sulfur atoms by selenium.

2. Outline of the linear muffin-tin orbital method in the atomic sphere approximation and the computational technique

The linear muffin-tin orbital method in the atomic sphere approximation (LMTO-ASA) energy-band method applied in our calculation has been described in [6, 7]. We outline here only those aspects pertinent to the present study. We perform a self-consistent band structure, because the self consistency is imperative for calculations of the ground-state properties of compounds. It includes the effect of charge transfer which is expected to provide the main uncertainty in energy-band calculation for compounds.

The ASA is used for the potential calculations. The total volume of the spheres around the atoms, where the potential is made spherically symmetric, is equal to the volume of the unit cell. Inside each atomic sphere, i.e. inside the sphere of type t ($t =$ S, P_t, Se) centred at q, the effective one-electron potential which we have used in the present calculations is:

$$V_t(r) = V_{Ht}(r) - \frac{2Z_t}{r} + V_{Mad,t} - V_{xc}(n_t(r)) \tag{1}$$

in atomic units. The first term is the Hartree potential or electron–electron repulsion obtained by solving Poisson's equation; the second term is the coulomb interaction between the electron and the nuclei; the third term is the Madelung potential which represents the interaction between the electron and the charge $z_{t'}$ centred on the other atomic spheres, where $z_{t'} = Z_{t'} - \int_{t'} n_{t'}(r)\,d\vec{r}$ integration extends over the sphere t' centred at $q' \neq q$). The last term is the exchange correlation potential is approximated, in our case, by the Barth–Hedin [8] local density approximation (LDA). The potential in the sphere enters only through the logarithmic derivative function $D_{\ell t}$ [6] or through a set of central parameters $C_{\ell t}$, $m_{\ell t}$, $a_{\ell t}$ and $b_{\ell t}$ defined by

$$[D_{\ell t}(E) - \ell + 1]^{-1} \approx [\tfrac{1}{2}\mu_{\ell t}S_t^2(E - C_{lt})]^{-1} + a_{\ell t} + b_{\ell t}S_t^2(E - C_{\ell t}) \tag{2}$$

where ℓ is the quantum number ($\ell = 0$, 1, 2) and S_t is the ASA radius of the tth atom. These four potential parameters are the basis for the procedure for carrying out the self-consistent band structure calculation.

The first step in the self-consistent procedure is to define the starting potential (or potential parameters) in each atomic sphere. First of all, we shall define the number and position of the ASA sphere in the unit cell. In fact, since the LMTO-ASA method is more efficient for closely packed structures [6], it is not directly applicable to open structures such as PtS_2, PtSeS and $PtSe_2$ which have a packing factor of only about 40% . So three empty spheres are inserted for each compound. The main effect of these empty spheres is to decrease the overlap between spheres centred at Pt, S and Se (this overlap, which is about 38%, decreases to 15% by the insertion of the empty spheres), which is imperative for this method, and also to decrease the number of iterations in the self-consistent procedure.

The atomic radii in PtS_2, PtSeS and $PtSe_2$ are obtained from the muffin-tin potential constructed according to the method suggested in [9] using Slater's free-electron exchange approximation. The electron density for neutral atoms are obtained by solving the Hartree–Fock–Dirac–Slater equation. The crossing point of the muffin-tin potential around the Pt and the chalcogene (S, Se) give the V_{MTZ} (V-muffin-tin zero) and the muffin-tin radii for Pt, S and Se. The structure data and V_{MTZ} for the three compounds are shown in table 1.

Our starting potential parameters used to perform the energy-band structure are obtained by solving the Dirac equation using the muffin-tin potential described above scaled to the relevant ASA radius. The projected state density and the state density have been obtained from the energy band calculated for a uniform mesh of 250 points in the irreducible wedge of the Brillouin zone by the tetrahedral method of integration [10]. The valence charge obtained from the radial function and the ℓ-projected state density added to the core charge density

Table 1. Structure data and V_{MTZ} of PtS_2, $PtSSe$ and $PtSe_2$.

		Compound		
		PtS_2	$PtSSe$	$PtSe_2$
Lattice parameters (a.u.)	a	6.635	6.786	7.045
(hexagonal unit cell)	c	9.508	9.568	9.602
Atomic coordinates		Pt(0,0,0)	Pt(0,0,0)	Pt(0,0,0)
		$S(\frac{1}{3}, \frac{2}{3}, u = 0.227)$	$S(\frac{1}{3}, \frac{2}{3}, u_1 = 0.227)$	$Se(\frac{1}{3}, \frac{2}{3}, u = 0.25)$
		$S(\frac{1}{3}, \frac{2}{3}, -u)$	$Se(\frac{2}{3}, \frac{1}{3}, u_2 = -0.25)$	$Se(\frac{2}{3}, \frac{1}{3}, -u)$
Empty sphere coordinates		$E(0, 0, 0.5)$	$E(0, 0, 0.5)$	$E(0, 0, 0.5)$
		$E_1(\frac{2}{3}, \frac{1}{3}, -\frac{1}{3})$	$E_1(\frac{1}{3}, \frac{2}{3}, -0.318)$	$E_1(\frac{2}{3}, \frac{1}{3}, -\frac{1}{3})$
		$E_1(\frac{1}{3}, \frac{2}{3}, \frac{1}{3})$	$E_2(\frac{2}{3}, \frac{1}{3}, 0.360)$	$E_1(\frac{1}{3}, \frac{2}{3}, \frac{1}{3})$
Atomic sphere radius (a.u.)		Pt = 2.616	Pt = 2.674	Pt = 2.757
		S = 2.427	S = 2.482	Se = 2.692
		S = 2.427	Se = 2.609	Se = 2.692
Empty sphere radius (a.u.)		E = 2.838	E = 2.728	E = 2.757
		E_1 = 2.047	E_1 = 2.139	E_1 = 2.065
		E_1 = 2.047	E_2 = 2.061	E_1 = 2.065
V_{MTZ} (Ryd)		−0.750	−0.701	−0.680

gives the total electron density in the corresponding atomic sphere. From the total electron density, we construct new atomic sphere potentials according to equation (1). The new set of potential parameters is generated from the ℓ-projected state density obtained above by means of canonical bands using energy scaling. The set of potential parameters obtained at the end of the scaling iterations is used to perform the energy-band calculation. The convergence criterion is that the change in the eigenvalues for the occupied band must be less than 2 mRyd between successive band iteration. Our calculation includes a combined correction for neglecting the corner of the atomic polyhedron and the higher partial waves. The eigenvalues are corrected to third order by perturbation theory.

The energies were evaluated at the following symmetry points Γ, A, K, H, L, M and along the symmetry line T, T′, S, S′, Δ, Σ and R of the Brillouin zone, derived from the hexagonal Bravais lattice.

3. Band structure and density of states

The self-consistent energy bands of PtSSe are shown in figure 1. Their total and partial densities of states are given in figure 2. The labelling of the different electronic levels is the standard labelling [11] deduced from the symmetry properties of Bloch sums formed from s, p and d orbitals around the Pt, S and Se.

The main result is that the energy-band structure of PtSSe obtained with the self-consistent LMTO-ASA energy-band approach, exhibits the semiconducting behaviour of PtSSe, with a gap less than that obtained for PtS_2, a fact which already reflects the effect of replacing of S by Se.

In the PtSeS compound 22 electrons in the unit cell (ten electrons from the Pt atom $5d^9 6s$, six electrons from S $3s^2 3p^4$ and six from Se $4s^2 4p^4$) fill the eleven electronic levels of the valence band, separated from the conduction band by a band gap (indirect electronic gap (IEG)) of about 0.64 eV. The main features of the band structure of PtSeS may be deduced from their partial densities and from the ℓ character of the electronic charge in the states corresponding to the different levels. The two low-lying electronic levels (VB1) have an almost 'pure' S 3s–Se 4s character. They are separated from the other bands by energy gap of
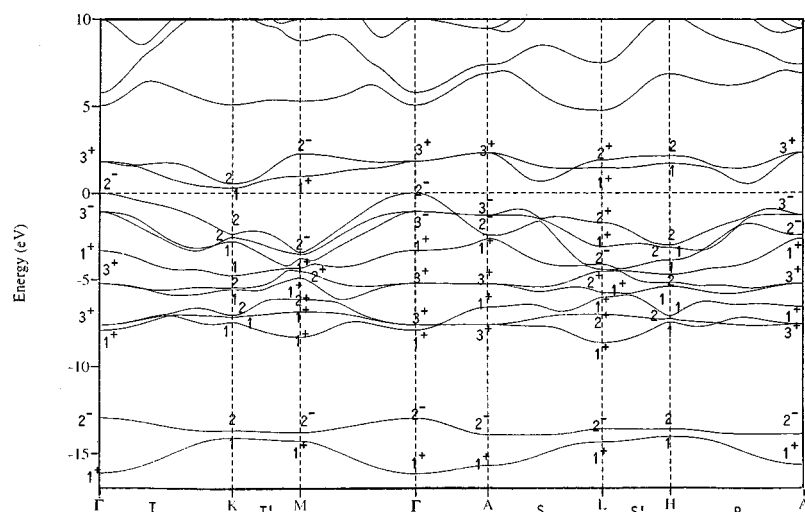
Figure 1. The self-consistent band structure of PtSSe without spin–orbit coupling.

about 5 eV. Such a result has been found for other transition metal dichalcogenides [12] and no significant variation for the other bands was observed in the band structure calculation of PdTe$_2$ with two grounds states $5s^2 5p^4$ and $5p^4$ for Te [13].

This fact shows the importance of the next six electronic levels (VB2) which are mainly derived from Pt 5d and chalcogene S 3p–Se 4p and the role played by these bands (p and d) when the Pt, S and Se are brought together to form the crystal PtSSe. In other words, the way in which these p and d bands mix together constitute the basis of the intra- and inter-layer bands as discussed below.

The conduction band, as the valence band, also presents two bands; the lower band (CB1) is derived mainly from Pt 5d and S 3p–Se 4p. The higher conduction band (CB2) is separated from CB1 by energy gap of about 3 eV. The metal 6p and 6s bands and the chalcogene bands (S 3d and Se 4d) are almost entirely confined in CB2. This fact is due to a strong hybridation between p and s bands of the metal and to highly-excited levels for S d and Se d. These levels occur both in the atom and in the solid.

In summary, the electronic-band structure of PtSSe presents four energy ranges separated by three energy gaps. The lower energy range is occupied by S 3s and Se 4s; the second energy range contains Pt 5d, S 3p and Se 4p; the third energy range contains S 3p, Se 4p and Pt 5d; and the higher energy range is occupied by Pt 6p, 6s, S 3d and Se 4d. We are only interested in the three lowest energy ranges.

This calculated band structure should reflect the main features of the PtSSe compound, in particular its lamellar character (intra-layer and inter-layer bonds) and the octahedral coordination of the chalcogene S–Se around the Pt. Before the detailed analysis of this band structure we could already relate the flat bands in a $\Gamma \rightarrow A$ direction to the layered character of the PtSSe compound.

From the ionic charge point of view, the transfer of four electrons from the platinum ($5d^9 6s^1$) to the chalcogene atoms, S ($3s^2 3p^4$) and Se ($4s^2 4p^4$), fills the p bands (p$_x$, p$_y$, p$_z$) of the sulfur and selenium and leaves the opportunity to have a gap between the d bands of platinum (d$_{x^2-y^2}$, d$_{xy}$, d$_{z^2}$, d$_{xz}$, d$_{yz}$), whereas the Pt s–p, and S 3d and Se 4d bands lie above these levels.
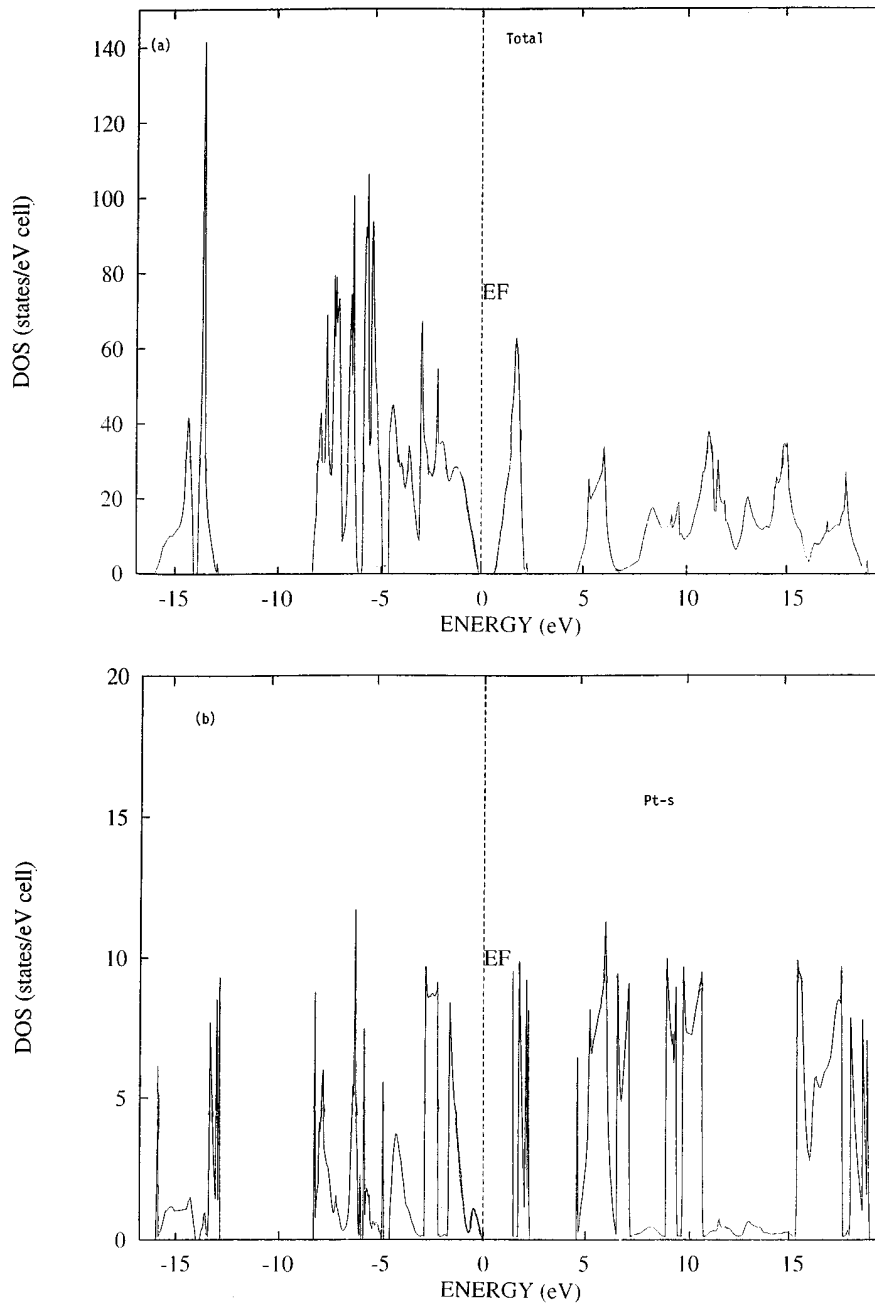
Figure 2. PtSSe total (a) and partial *l*-projected ((b)–(j)) densities of states functions: (b), Pt s, (c), Pt p; (d), Pt d; (e), S s; (f), S p; (g), S d; (h), Se s; (i), Se p; and (j), Se d.

Nevertheless, the proximity of the binding energy E_p for S–Se and Ed for Pt in neutral atoms yields, in the compound we studied (see VB2), a strong overlap and, probably, a covalent bonding effect between the metal d and chalcogene p orbitals,
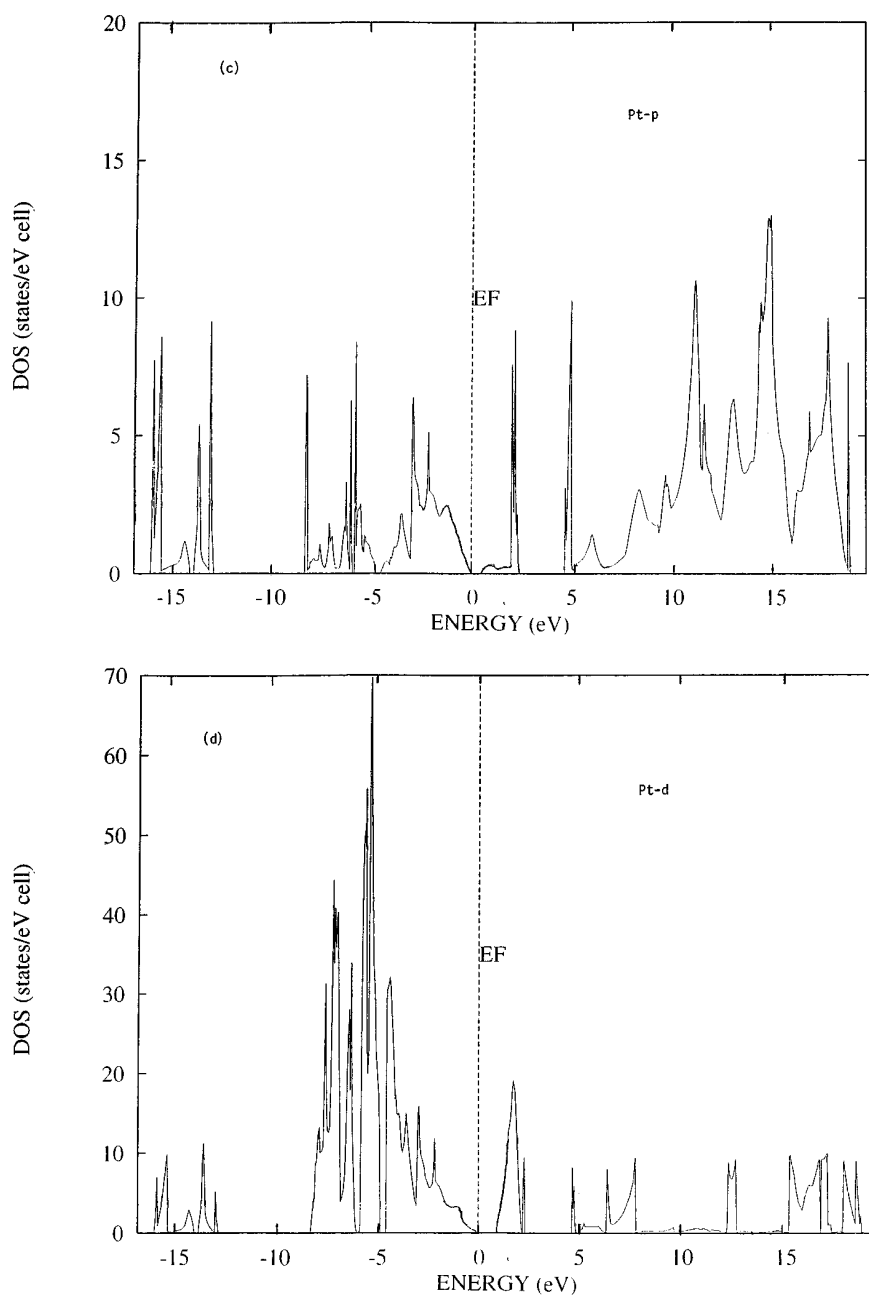
Figure 2. (Continued)

which results in the formation of chalcogene metal d/p and chalcogene bonding and antibonding states. The remaining filled d levels lie between these states. A symmetrical analysis combined with the percentage analysis of the wavefunction and from [14] justify the characterization of the Γ^{3+} (-5 eV) and Γ^{1+} (-3.3 eV) levels (relative to the ε_F (Fermi level)) as remaining filled d levels, with wavefunctions $d_{x^2-y^2}$, d_{xy} and
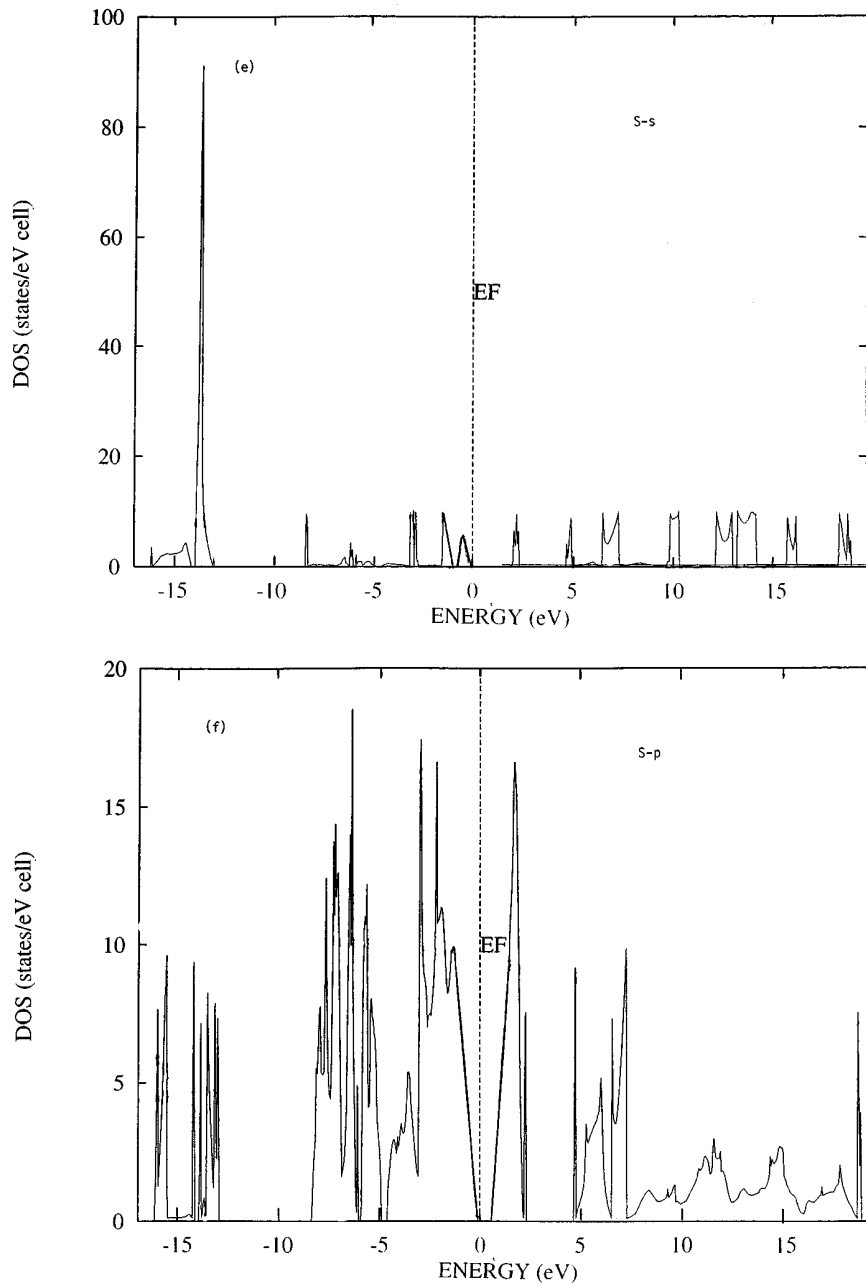
Figure 2. (Continued)

d_{z^2} respectively. Such orbitals or non-bonding orbitals serve only to accommodate electrons. We can also find non-bonding orbitals in other materials, such as amorphous Si [15].

The level Γ^{3+} (−7.2 eV) contains almost the same contribution of metal d orbital and chalcogene p orbital, and the d_{xz}, d_{yz} and p_{xy} already point in the bond direction. We are
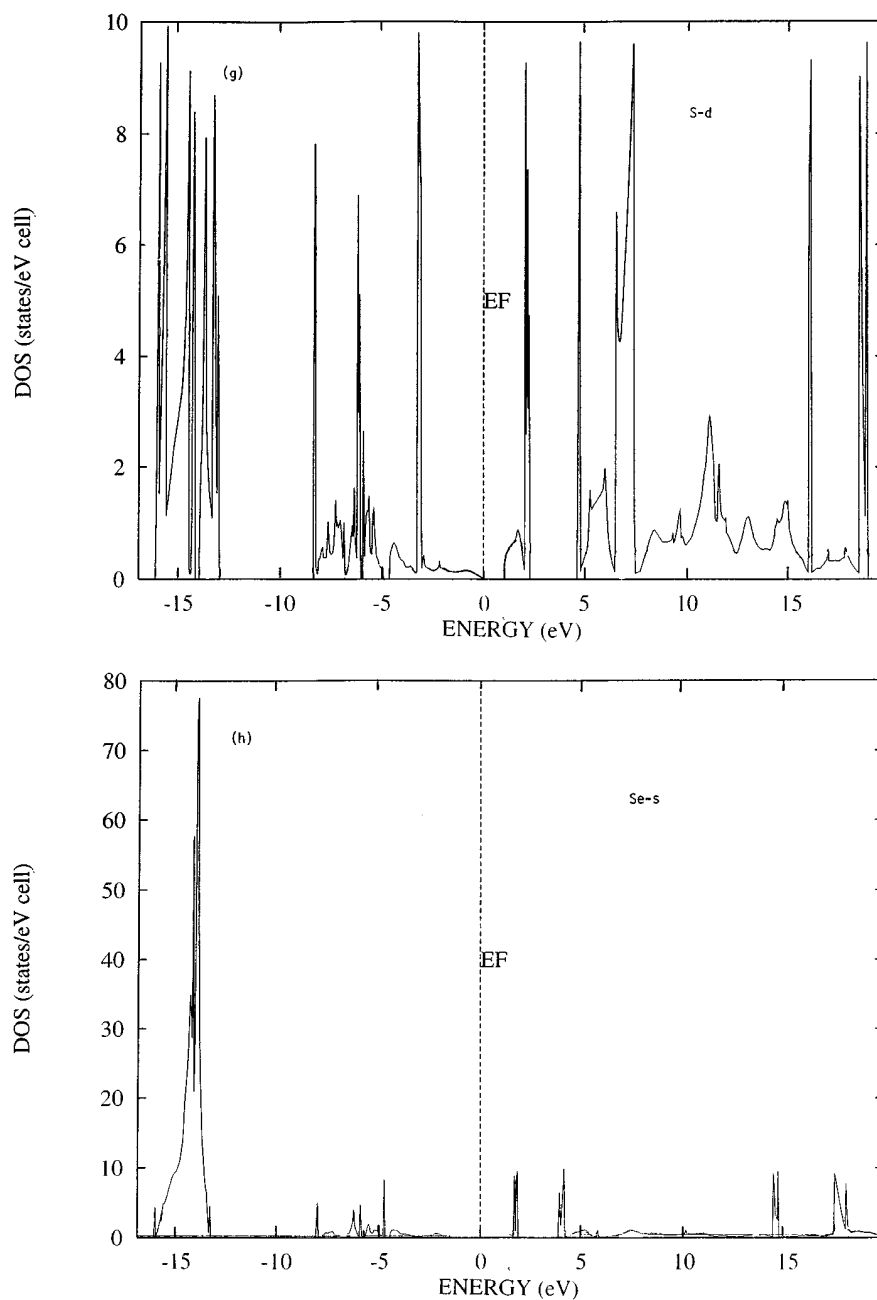
Figure 2. (Continued)

led to define this level as the bonding state with a wavefunction $(d_{xz}, d_{yz}/(p_{xy})^+)^+$ and the antibonding state as $(d_{xz}, d_{yz}/(p_{xy})^-)^-$ for Γ^{3+} (1.8 eV) that lies above the Fermi level.

So the nature of the intra-layer bond depends on this bonding state. For the PtSSe, compound, the intra-layer bonds presents a covalent character, as consequence of the overlap between Pt (d_{xz}, d_{yz}) orbitals (50%) and S–Se $((p_{xy})+)$ orbitals (50%). Such a high overlap
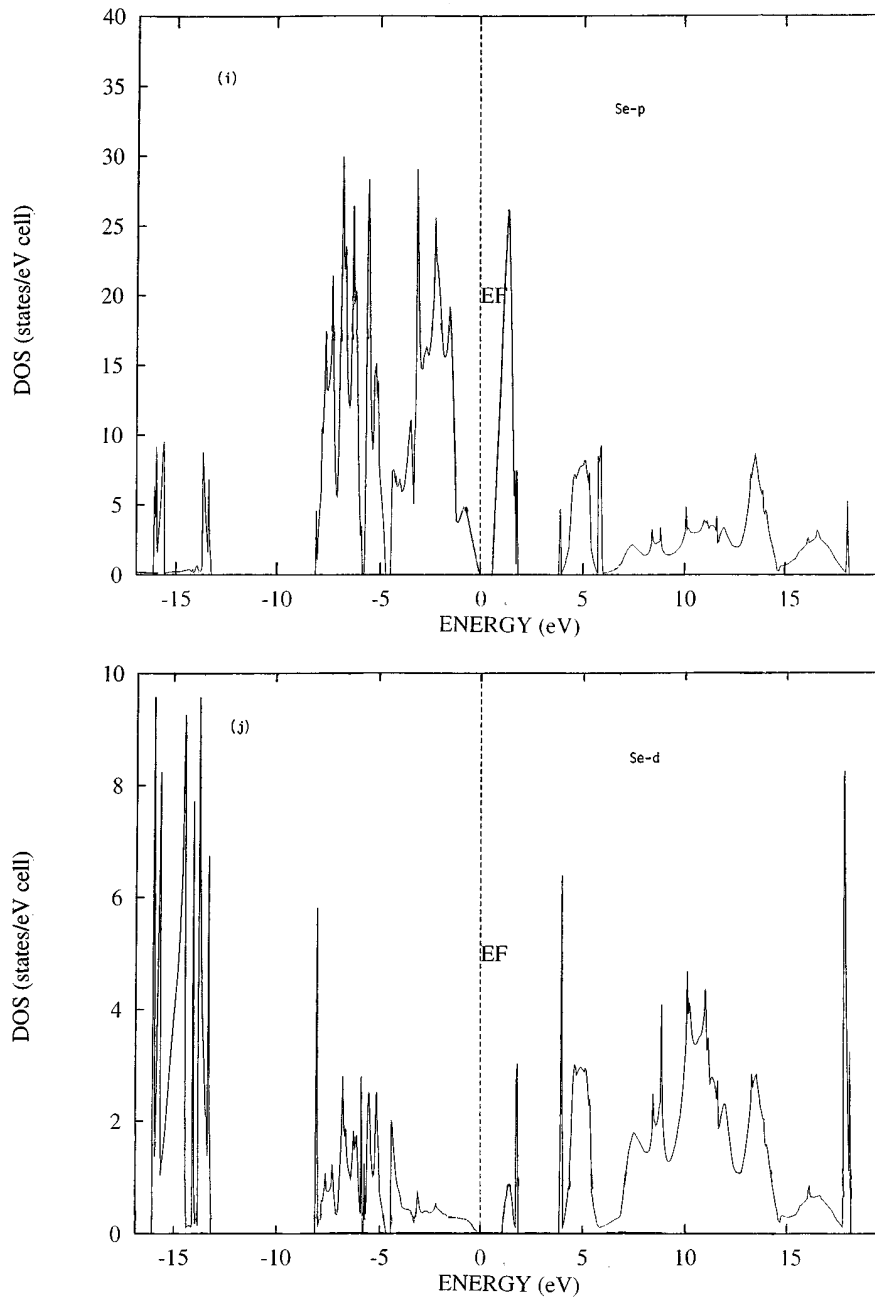
Figure 2. (Continued)

arises because the distance between anion planes (2.41 Å) is less than the sum of the ionic radius $S_e^{2-} + S^{2-}$ (3.82 Å), which is a consequence of the departure of the PtSSe crystal structure ($c/a = 1.41$) from an ideal close packing ($c/a = 1.63$).

The symmetry analysis excludes any contribution of the metal d orbital to the bonding $(p_z)^+$ and antibonding $(p_{xy})^-$ and $(p_z)^-$ states between S and Se. These states correspond, respectively, to the energies Γ^{1+} (-7.9 eV), Γ^{3-} (-1.09 eV) and Γ^{2-} (0 eV).
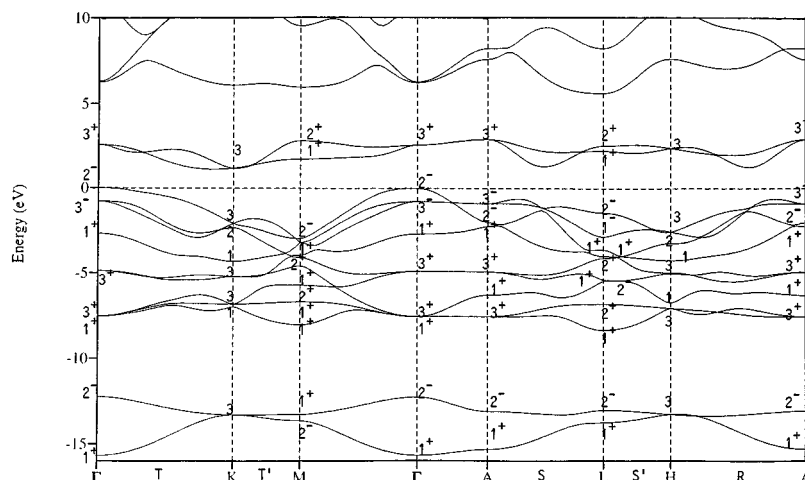
Figure 3. Self-consistent band structure of PtS_2 without spin–orbit coupling.

The state $(p_z)^-$ is very sensitive to a variation of $z(u_1, u_2)$ (table 1) the layer height parameter. Since an increase of u_1 and u_2 yields a decrease of the d_{s-se} inter-layer and to a slower increase of $d_{pt-s,se}$ and d_{s-se} intra-layers, we expected that the state $(p_z)^-$ has a pronounced inter-layer character. A similar conclusion was reached in the band structure of the layer compounds ZrS_2, TeS_2 and $TiSe_2$ [16]. From the valence band picture [14], each chalcogenide atom, Se or S, puts a lone pair of electrons into the van der Waals region. The electronic charge in the different spheres at the end of the self-consistent procedure $(C_{Pt} = 9.67\ e,\ C_{s,se} = 1.66\ e;\ C_E = 1.00\ e;\ C_{E1} = 0.526\ e;\ C_{E2} = 0.465\ e)$ shows a charge transfer from the chalcogenide atoms into this region. Hence the inter-layer bond can be considered, similar to the case of an inert gas, as an interaction between two 'neutral atoms', each with the ground state $(np_z^-)^2$ and with a completely filled electron shell. Its strength depends on the distance between the two 'neutral' atoms.

Filling these levels with the available electrons of the constituent atoms (Pt, S or Se) we get a semiconductor with indirect gap about 0.64 eV between Γ^{-2} and K^1.

4. Effect of anion substitution in the sequence $PtS_2 \rightarrow PtSSe \rightarrow PtSe_2$

As PtSSe, PtS_2 and $PtSe_2$ are layer compounds which crystallize with the CdI_2 structure, they are reported to occur as strongly bonded, two-dimensional (S–Pt–S and Se–Pt–Se) layers with weak interlayer coupling. Each Pt atom is surrounded by six nearest neighbour metal atoms and the coordination of the chalcogene around the platinum is octahedral [5]. Single crystals were prepared by chemical vapour transport and are obtained as platelets which are easily peeled in the direction perpendicular to the layers.

The self-consistent band structures of PtS_2 and $PtSe_2$ are shown figures 3 and 4, respectively. These band structures predict semiconducting behaviour for PtS_2 with an indirect optical gap ($\Gamma^{-2} \rightarrow$ K) about 1.35 eV [17] for the former and a semi-metallic behaviour, with a slight indirect overlap between a valence band VB2 and a conduction band CB1, for the latter [5, 18]. For the sake of simplicity, we shall continue to use VB2 and CB1 for $PtSe_2$, keeping in mind the slight overlap between them, except when the semi-metallic behaviour of the compound is considered.
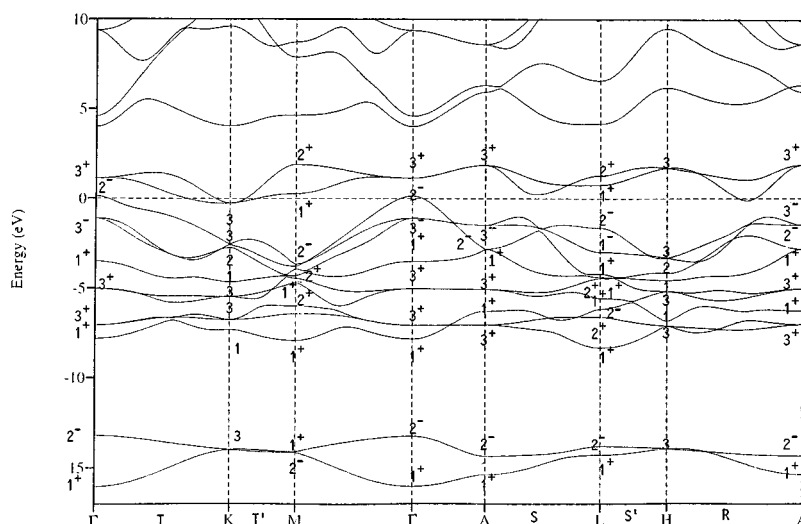
Figure 4. Self-consistent band structure of PtSe$_2$ without spin–orbit coupling.

From the chemical formulae these three compounds, in going from PtS$_2$ → PtSSe → PtSe$_2$, differ from each other only by the sequential substitution of one sulfur atom by a selenium atom. However, the replacement of only one anion is sufficient to change their lattice constants and their 'electrical properties'. In fact, for this sequence PtS$_2$ → PtSSe → PtSe$_2$, the lattice constants a and c increase from left to right, while the IEG decreases and leads to the semi-metallic behaviour of PtSe$_2$.

These changes in the lattice constants, a and c, is probably due to the fact that the anionic radius of Se^{2-} (1.98 Å) is greater than the anionic radius of S^{2-} (1.84 Å). The variation of the IEG is less clear and reflects, in some way, a delocalization of the electrons even though these three compounds are iso-electronic (the same number of valence electrons) and the comparison between their band structure, performed by the same method (LMTO-ASA) shows a qualitative similarity.

In fact, the band structure for each of these materials presents four energy ranges (VB1, VB2, CB1 and CB2) separated by three energy gaps and each energy range is occupied by the same orbitals (see discussion in section 2) and the shape of the sub-bands are almost the same (except the band structure of PtSe$_2$ which presents only three energy ranges).

It is immediately clear that the ground-state energy spectra are qualitatively equal along this sequence, with only a minor difference. Due to lowering in group symmetry for PtSSe compared to those of PtS$_2$ and PtSe$_2$, its electronic levels are no longer degenerate in symmetry points K and H. Moreover a small increase of the energy gap VB2–VB1 is observed in the sequence PtS$_2$ (4.5 eV) → PtSSe (5 eV) → PtSe$_2$ (5.5 eV).

Above the Fermi level ε_F, the situation is quite different, the two groups CB1 and CB2 move closer to the Fermi level, almost linearly, leading to the decrease of the IEG. The decrease of the gap and the increase of the band width (PtS$_2$ → PtSSe → PtSe$_2$) is attributed to the decrease of the correlation energy. Such an effect has been studied in the band structure of Mg [19] and LiF [20].

A closer examination, however, reveals distinct qualitative differences. In particular, the relative position of the energy of the levels in the VB2 bands are quite different from one compound to another, but the corresponding wavefunction remains of the same type and

contains the same percentage of electronic charge, and for $PtSe_2$, for example, the level around Γ^{-2} increases to the Fermi level, whereas the levels around K^3 and R repel in VB2. Such effects are due to a redistribution of the electronic charge, which may be explained, not only by the difference between the size of the ionic radii of S and Se, but also by the difference of their electronegativity ($el_S = 2.5$; $el_{Se} = 2.4$). A comparison between the electronic charge in the empty sphere at the end of the self-consistent procedure confirms such redistribution.

The total charge in E, E_1 and E_2 remains almost about 2 e for the three compounds, but changes in the same sphere from one compound to another. The constancy of the electronic charge shows that the process of interaction between one layer the next is quite similar for the three compounds (see discussion in section 2). It seems that the increase, from PtS_2 to $PtSe_2$, of the overlap between the 'neutral' atoms, which is forbidden by the Pauli exclusion principle, yields the transfer of the electronic charge from the occupied state $(p_z)^-$ to the unoccupied antibonding state $(d_{xz}, d_{yz}/(p_{xy})^-)^-$, leading to a slight overlap between the valence and conduction bands for $PtSe_2$. Therefore, the electrical properties of layered compounds can be related to the interaction between two interlayers chalcogenide atoms.

At this point we note that it is from the results of the electronic structure calculations on PtS_2, PtSSe and $PtSe_2$ within the LMTO-ASA that we draw conclusions on the effect of anion substitutions in PtS_2, and we have discussed these results in terms of charge transfer and coordination effects. Therefore, our conclusions and discussions depend on the technique (LMTO-ASA) from which these results are obtained and its ability to yield reliable results. The choice of this method is not haphazard and it is justified by the fact that it has been successfully used for similar compounds, such as SnO_2, GeO_2, TeO_2 [21], MoS_2 [2] and $NiTe_2$, $PdTe_2$, $PtTe_2$ [22]. Most importantly, its reliability has already been tested; our experimental results on PtS_2 [3] are well interpreted with the electronic structure calculation on PtS_2 within the LMTO-ASA using the LDA [17].

5. Conclusions

We have calculated the energy-band structure and its corresponding total and partial densities of states of the compound PtSSe, using the self-consistent LMTO-ASA. The energy-band structure obtained predicts the semiconducting behaviour of PtSSe, with an indirect band gap of about 0.64 eV between Γ^{2-} and K^1 and reflects its lamellar structure; the intra-layer bonds described by the bonding state $(d_{xz}, d_{yz}/(p_{xy})^+)^+$ present a covalent character and the adjacent layers are held together by the van der Waals forces described by the antibonding state $(p_z)^-$.

We believe that a replacement of S by Se in the sequence $PtS_2 \rightarrow$ PtSSe $\rightarrow PtSe_2$ yields a variation of the lattice constants, combined with a redistribution of the 'electronic charge'. The two effects contribute to preserve the covalent character of the intra-layer bonds and the weak coupling by the van der Waals interlayer forces. The electrical properties of the layer compounds depend on the strength of the later interaction. We have not found any charge transfer from the anions to the cation.

References

[1] Pearson W B 1967 *A Handbook of Lattice Spacing and Structures of Metals and Alloys* (Oxford: Pergamon)
[2] Kasowski R V 1973 *Phys. Rev. Lett.* **30** 1175
[3] Mankai C, Martinez G and Gorochov O 1977 *Phys. Rev.* B **16** 4666
[4] Kliche G 1984 *J. Solid State Chem.* **001** 3140
[5] Soled S, Wold A and Gorochov O 1976 *Mater. Res. Bull.* **11** 927
[6] Anderson O K 1975 *Phys. Rev.* B **12** 3060
[7] Skriver H L 1984 *The LMTO Method* (Heidelberg: Springer)
[8] Barth U and Hedin L 1972 *J. Phys. C: Solid State Phys.* **5** 1629
[9] Loucks T L 1967 *Augmented Plane Wave Method* (New York: Benjamin)
[10] Jepsen O and Anderson O K 1971 *Solid State Commun.* **9** 1763
[11] Slater J C 1965 *Quantum Theory of Molecules and Solids* (New York: McGraw-Hill)
[12] Schluter I Ch and Schluter M 1973 *Phys. Status Solidi* **57** 145
[13] Jan J P and Skriver H L 1977 *J. Phys. F: Met. Phys.* **7** 1719
[14] Wilson J A and Yoffe A D 1969 *Adv. Phys.* **18** 193
[15] Brodsky M H 1979 *Amorphons Semiconductors* (Berlin: Springer)
[16] Isomäki H and Von Boehm J 1977 *Il Nuovo Cimento* **38 B** 168
[17] Mankaï C and Bennaceur R 1988 *J. Phys. C: Solid State Phys.* **21** 4979
[18] Guo G Y and Liang W Y 1986 *J. Phys. C: Solid State Phys.* **19** 995
[19] Asokamani R and Iyakutti K 1978 *J. Phys. F: Met. Phys.* **8** 2323
[20] Zunger A and Freeman A J 1977 *Phys. Rev.* B **16** 2901
[21] Savane A and Antoncik E 1987 *J. Phys. Chem. Solids* **48** 171
[22] Guo G Y and Liang W Y 1986 *J. Phys. C: Solid State Phys.* **19** 5365